

# The first month of evolution of the slow rising type II-P SN 2013ej in M74\*

S. Valenti<sup>1,2</sup> †, D. Sand<sup>3</sup>, A. Pastorello<sup>4</sup>, M. L. Graham<sup>1,2</sup>, D. A. Howell<sup>1,2</sup>, J. Parrent<sup>1,5</sup>, L. Tomasella<sup>4</sup>, P. Ochner<sup>4</sup>, M. Fraser<sup>6</sup>, S. Benetti<sup>4</sup>, F. Yuan<sup>7</sup>, S. J. Smartt<sup>6</sup>, J. R. Maund<sup>6</sup>, I. Arcavi<sup>8</sup>, A. Gal-Yam<sup>8</sup>, C. Inserra<sup>6</sup>, D. Young<sup>6</sup>

<sup>1</sup> Las Cumbres Observatory Global Telescope Network, 6740 Cortona Dr., Suite 102, Goleta, CA 93117, USA

<sup>2</sup> Department of Physics, University of California, Santa Barbara, Broida Hall, Mail Code 9530, Santa Barbara, CA 93106-9530, USA

<sup>3</sup> Physics Department, Texas Tech University, Lubbock, TX 79409, USA

<sup>4</sup> INAF Osservatorio Astronomico di Padova, Vicolo dell’Osservatorio 5, 35122 Padova, Italy

<sup>5</sup> Department of Physics and Astronomy, Dartmouth College, 6127 Wilder Laboratory, Hanover, NH 03755, USA

<sup>6</sup> Astrophysics Research Centre, School of Mathematics and Physics, Queens University Belfast, Belfast BT7 1NN, UK

<sup>7</sup> Research School of Astronomy and Astrophysics, The Australian National University, Weston Creek, ACT 2611, Australia

<sup>8</sup> Department of Particle Physics and Astrophysics, The Weizmann Institute of Science, Rehovot 76100, Israel

Accepted ....; Received ....; in original form ....

## ABSTRACT

We present early photometric and spectroscopic observations of SN 2013ej, a bright type IIP supernova in M74. SN 2013ej is one of the closest SNe ever discovered. The available archive images and the early discovery help to constrain the nature of its progenitor. The earliest detection of this explosion was on 2013 July 24.14 UT and our spectroscopic monitoring began on July 27.73 UT, continuing almost daily for two weeks with the LCOGT FLOYDS spectrographs. Daily optical photometric monitoring was achieved with the LCOGT 1m network, and were complemented by UV data from *SWIFT* and near-infrared spectra from PESSTO and IRTF. The data from our monitoring campaign show that SN 2013ej experienced a 10-day rise before entering into a well defined plateau phase. This unusually long rise time for a type IIP has been seen previously in SN 2006bp and SN 2009bw. A relatively rare strong absorption blue-ward of H $\alpha$  is present since our earliest spectrum. We identify this feature as Si II, rather than high velocity H $\alpha$  as sometimes reported in the literature.

**Key words:** supernovae: general – supernovae: SN 2013ej

## 1 INTRODUCTION

Type IIP supernovae (SNe) have been widely studied in the past. They arise from progenitors that have retained their hydrogen and helium layers before exploding as core-collapse (CC) SNe. Several progenitors of type IIP SNe have been detected in archive images (see Smartt 2009, for a review). These SNe are also used as standard candles for cosmological studies (Hamuy 2001). For this reason it is important to investigate their diversity when new close-by type II SNe are discovered. We have this opportunity with SN 2013ej, a young SN recently discovered in M74 (NGC 628).

SN 2013ej was discovered by the Lick Observatory Supernova Search (LOSS) on 2013 July 25.45 UT, with the 0.76-m Katzman Automatic Imaging Telescope (KAIT). The coordinates of the SN are  $\alpha = 01h36m48.16s$ ,  $\delta = +15^\circ45'31.0''$  (Kim et al. 2013). Pre-discovery detections on July 25.38 and on July 24.125 were also reported by Dhungana et al. (2013) with the 0.45-m ROTSE-IIIb telescope at McDonald Observatory and by C. Feliciano on the *Bright Supernovae*<sup>1</sup> web site. The SN was caught extremely young, as a non-detection was reported by the All Sky Automated Survey for SuperNovae

\* This paper is based on observations obtained with the following telescopes: LCOGT Network of 1m and 2m Telescopes, NTT(184.D-1140,188.D-3003), IRTF

† e-mail: svalenti@lcogt.net

<sup>1</sup> <http://www.rochesterastronomy.org/snimages/>

(ASAS-SN, Shappee et al. 2013) on July 23.54 UT<sup>2</sup>, less than one day prior to the first detection, with a limit (though not very stringent) of  $V > 16.7$  mag. We immediately triggered the robotic FLOYDS spectrograph mounted on the Faulkes Telescope South (FTS) at Siding Spring Observatory and were able to classify the transient on Jul. 27.70 UT as a young type II SN (Valenti et al. 2013). Located 92°.5 E, 135° S from the core of M74<sup>3</sup>, SN 2013ej is a very nearby SN. We note that M74 hosted two other CC SNe, viz. SN 2002ap (SN Ic) and SN 2003gd (SN IIP).

Deep, high resolution images of the host galaxy have been taken prior to the explosion of SN 2013ej using the Hubble Space Telescope (HST) and Gemini telescope. An analysis of these together with the identification and characterization of a progenitor star is presented in a companion paper (Fraser et al. 2013). A bright source in both the HST and Gemini images is identified by Fraser et al. (2013) as coincident with the position of SN 2013ej. The object is detected from the  $U$  to the  $i$  bands and does not have the colours of a single stellar source. Fraser et al. (2013) show that it is likely a blend of two, physically unrelated, stars and that the progenitor was consistent with a red supergiant.

For the reasons mentioned above, SN 2013ej was promoted as a high priority target for LCOGT's ongoing, intensive effort to obtain high cadence optical photometry and spectroscopy of transient objects. A detailed overview of the LCOGT facilities can be found in Brown et al. (2013). Along similar lines, SN 2013ej was also monitored by the PESSTO<sup>4</sup> collaboration.

## 2 OBSERVATIONS

Spectroscopic followup of SN 2013ej was primarily obtained using the twin FLOYDS spectrographs on FTS and the Faulkes Telescope North (FTN), at Haleakala, with a  $\sim 1$  day cadence. FLOYDS has a prism cross-disperser which images first and second orders onto the chip, resulting in a very broad wavelength coverage of  $\sim 3200\text{--}10000\text{\AA}$ . Optical spectra were also obtained at the Asiago 1.22m telescope with the B&C spectrograph. All optical spectra were reduced using standard IRAF routines. A higher resolution spectrum was obtained on August 23rd with the 1.82m Copernico Telescope (Mt. Ekar, Asiago) equipped with an echelle spectrograph. Two near-infrared (NIR) spectra were also collected. A very early NIR spectrum (taken earlier than our first optical spectrum) was obtained with SpeX (Rayner et al. 2003) on the NASA Infrared Telescope Facility (IRTF). The SpeX data were reduced with the custom Spextool package (Cushing, Vacca & Rayner 2004), and were corrected for telluric absorption with the software and prescription of Vacca, Cushing & Rayner (2003). SOFI data were obtained during a PESSTO night and reduced with the PESSTO pipeline (Smartt et al. in prep.) (data available online (Tab. 1 and Tab. 2)

Optical ( $UBVRIgriz$ ) photometric follow-up of SN 2013ej was obtained with the nine 1-m telescopes of the LCOGT network, and in this paper we present data obtained up to one month after the SN discovery. The data were reduced using a custom pipeline<sup>5</sup> developed by the LCOGT SN team. Additionally, *SWIFT* target of opportunity observations of SN 2013ej with the Ultraviolet/Optical Telescope (UVOT; Roming et al. 2005) were taken starting on 2013 July 30.87 UT. *Swift* photometry, going from the  $uw2$  filter ( $\lambda_c=1928\text{\AA}$ ) through the  $V$  filter ( $\lambda_c=5468\text{\AA}$ ), has been measured using an aperture of 3'', and following the approach of Brown et al. (2009).

## 3 ANALYSIS AND RESULTS

### 3.1 Spectroscopy

The sequence of spectra collected for SN 2013ej is shown in Fig. 1a. In analogy with canonical type II SNe, at very early phases the spectra of SN 2013ej show a blue, almost featureless continuum. As the ejecta expand, the photospheric temperature declines, and a number of spectral lines appear, showing P-Cygni profiles that become more prominent with time. The earliest spectrum shows a blue continuum, with a black body temperature of 15000 K. Together with weak and shallow Balmer-series lines, N II and He I likely contribute to the absorption features at 5550 Å and 5700 Å. From very early phases, an absorption feature on the blue side of H $\alpha$  is detected (see Fig. 1c). This feature, observed in several young SNe II, has been widely discussed in the past, particularly for the classic type IIP SN 1999em. The two identifications proposed to explain the dip are a high velocity (HV) component of H $\alpha$  (at  $\sim 16,000 \text{ km s}^{-1}$ ) or, alternatively, Si II 6355 Å. The evolution of this feature has been observed in several IIP SNe (SN 2005cs, Pastorello et al. 2006; SN 2006bp, Quimby et al. 2007; SN 2009bw Inserra et al. 2012 and SN 2012A, Tomasella et al. 2013). It appears a few days after shock break-out, it reaches a maximum intensity at around three weeks after maximum light before eventually fading. In Fig. 1d spectra at these three different epochs of SN 2013ej are compared with those of other SNe IIP (a few days, 2 weeks and 3–4 weeks after the explosion respectively). In SN 1999em this absorption was visible since about one week post-explosion, and remained detectable for one additional week. Leonard et al. (2002) identified this absorption at early phases as Si II, while Baron et al. (2000) favoured a HV hydrogen interpretation. Inserra et al. (2012) also interpreted this feature as a high velocity hydrogen line in the type II SN 2009bw. Chugai, Chevalier & Utrobin (2007), on the other hand, proposed a time dependent, dual interpretation. These authors

<sup>2</sup> We will use this epoch (JD=2456497.0±1.0) as the reference date for the shock breakout

<sup>3</sup> A distance modulus of 29.79 mag (Fraser et al. in prep.), or 9.1 Mpc, is used in this paper.

<sup>4</sup> Public ESO Spectroscopic Survey of Transient Objects, [www.pessto.org/](http://www.pessto.org/)

<sup>5</sup> The pipeline employs standard procedures (*pyraf*, *DAOPHOT*, *SWARP*) in a python framework. Point-spread function instrumental magnitudes were transformed to the standard Sloan Digital Sky Survey (SDSS) filter system (for *ugriz*) or Landolt (1992) system (for *UBVRI*) via standard star observations taken during clear nights.

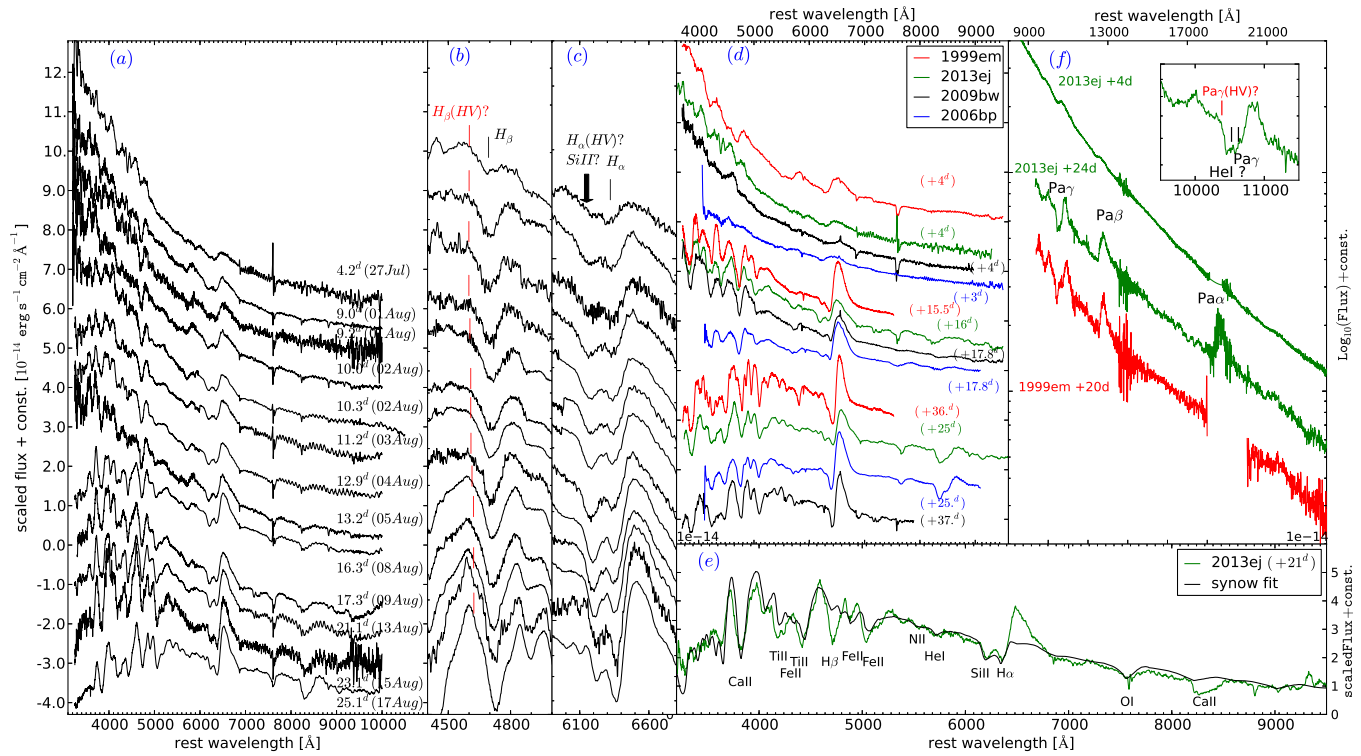


**Figure 1.** (a): Spectra series of SN 2013ej. (b):  $H\beta$  evolution; (c)  $H\alpha$  evolution; (d): Comparison of spectra of SN 2013ej with those of other SNe II at three different epochs. (e): Line identification: comparison between an observed spectrum of SN 2013ej (phase +20<sup>d</sup>) and a spectral model obtained using *synow* (see text). (f): Infrared spectra of SN 2013ej and comparison with an early-phase spectrum of SN 1999em. The insert shows a detail of  $\text{Pa-}\gamma$ .

attributed the shallow absorption in the  $H\alpha$  blue wing visible at early phases in SNe type IIP to  $\text{Si II}$ , but a similar blue-shifted notch seen at late times to HV hydrogen. Indeed, the interaction with a typical red supergiant wind should result in the enhanced excitation of the outer layers of unshocked ejecta and the emergence of corresponding HV absorption (see also Leonard et al. 2002, for a similar conclusion). In the case of SN 2013ej, we note a similar evolution of this absorption feature to previous works, although a notch is visible in our first spectrum and becomes stronger with time. At day +17 the blue-shifted absorption is deeper than the regular  $H\alpha$  absorption. We also note that a similar feature is not visible in the blue wing of  $H\beta$  (see Fig. 1b), as one would expect if it is due to HV hydrogen.

In order to confidently exclude the HV H interpretation for the 6100 Å feature, we also present in Fig. 1f two NIR spectra obtained on July 27th and August 17th. The first SpeX spectrum (+ 4<sup>d</sup>) is one of the earliest NIR spectra ever published for a SN type IIP. This shows a blue continuum, in addition in which only very shallow Paschen lines are detected. These become more prominent in the second spectrum, and show a broad absorption in  $\text{Pa-}\gamma$  (see inset of Fig. 1f). While the red wing of the absorption is consistent with  $\text{Pa-}\gamma$  at  $\sim 8000 \text{ km s}^{-1}$  consistent with other hydrogen lines, the origin of the blue wing of this feature must wait for future work with time-series NIR spectroscopy. HV  $\text{Pa-}\gamma$  at  $\sim 15000 \text{ km s}^{-1}$  (as suggested by the HV hydrogen identification in the optical) can be excluded.

A *synow* (Fisher 2000) fit of the spectrum at 21 days is shown in Fig. 1e, and the comparison model was obtained with the following contributing ions:  $\text{Fe II}, \text{Ti II}, \text{He I}, \text{H I}, \text{O I}, \text{Si II}, \text{Ca II}, \text{N II}$ . The  $H\beta$  feature is not well reproduced because of the non-LTE condition of the H-rich layers. Enhancing the optical depth of  $\text{H I}$  may help improving the match with the observed profile of  $H\beta$ , but this would make the  $H\alpha$  absorption too prominent. Adding  $\text{Si II}$  nicely reproduces the feature on the blue side of  $H\alpha$  with no significant change in the *synow* spectrum due to other  $\text{Si II}$  lines. Also remarkable are the  $\text{Fe II}$  lines, first detected when the temperature goes below 9000 K, (as suggested by Dessart & Hillier (2006)). In particular, the  $\text{Fe II}$  line at 5166  $\lambda\lambda$  appears two weeks after the core-collapse and is clearly detected one week later. In Fig. 2a we show the photospheric velocity where lines of different ions are forming. The velocity obtained for the  $\text{Si II}$  identification is also consistent with those of other elements.

### 3.2 Light curve

The light curve of SN 2013ej in the *uw2,um2,uw1,UBVRIGrizj* filters is shown in Fig. 2b. SN 2013ej shows in all bands a relatively slow luminosity rise to the plateau. SNe II usually have a very fast rising lasting very few days. Through the

comparison of the early light curve of SN 2010id with that of SN 2006bp (Quimby et al. 2007), Gal-Yam et al. (2011) suggested a variety in the rising time of type II SNe, with some objects showing a slow rise. Another SN II with a slow rise to peak is SN 2009bw (Inserra et al. 2012). These three SNe are all quite bright ( $M_R$  between -17 and -18 at peak (see Fig. 2c). In particular, SN 2009bw is almost identical to SN 2013ej in the light curve shape and the absolute magnitude (see Fig. 2b). The rise time for type II SNe is usually connected to the radius of the progenitor at the time of its explosion. The slower the rise time, the more compact the progenitor. However the temperature evolution of SN 2013ej (Sect. 3.1) seems to favour an extended progenitor.

### 3.3 Progenitor Radius

In core-collapse SNe, soon after the shock break-out, the shock-heated envelope expands and cools down with different time scales depending on the initial progenitor radius, opacity and gas composition. Simple analytic functions have been developed (Waxman, Meszaros & Campana 2007; Rabinak & Waxman 2011; Chevalier & Irwin 2011) to give a rough estimate of the radius of the progenitor of core-collapse SNe using the temperature evolution at early phases. For instance, the SN photosphere after the explosion of a red supergiant (RSG) remains at a higher temperature for a longer time than what occurs in a more compact blue supergiant (BSG). Making use of our spectro photometric data within one week from the shock-breakout and the eq. 13 of Rabinak & Waxman (2011), we constrained the radius of the exploding star. With an optical opacity of  $k=0.34 \text{ cm}^2 \text{ g}^{-1}$  the temperature evolution of SN 2013ej is consistent with that of a progenitor with radius  $400\text{-}600 R_\odot$ .

We remark that no host reddening was assumed in this calculation of the progenitor radius, which is consistent with the lack of NaID lines at the redshift of M74 in the echelle spectrum obtained with the 1.82m Asiago telescope (see Fig. 3b). With the addition of some host reddening, the temperature and consequently the radius estimates would be larger. The likely RSG progenitor star identified by Fraser et al. (2013) has a luminosity of  $\log L/L_\odot = 4.5 - 4.9$  dex, which would imply radii of  $400\text{-}800 R_\odot$  for M-type supergiant stellar effective temperatures. These radii are also consistent with that of the type IIP SN 2009bw (Inserra et al. 2012), which shares several other characteristics with SN 2013ej, as we will discuss in the next section.

The inferred radius values should be confirmed with more detailed models, but here we may safely conclude that the temperature evolution of SN 2013ej is consistent with that expected in the explosion of an extended progenitor. In Fig. 3a we also present progenitor radius constraints for SN 2013ej utilizing our *SWIFT* and optical broadband photometry, which generally agree with our spectroscopic results. We note that the temperature evolution inferred using the *SWIFT* data is always lower than that derived from the optical data, suggesting that some UV line blanketing is already present at very early phases. We further compare the temperature evolution of SN 2013ej with those of other type II SNe. The photospheric temperatures and radii of SN 2013ej are similar to those of SN 2009bw and SN 2012A, while they are always higher than those of SN 1987A.

## 4 DISCUSSION AND CONCLUSION

In this letter we present the early photometric and spectroscopic evolution of SN 2013ej, a luminous type II SN that exploded in the very nearby spiral galaxy M74. Data were obtained mostly with the 1m and 2m telescopes of the LCOGT network, complemented with data from the PESSTO collaboration. The most interesting characteristic of our sequence of early-time spectra of SN 2013ej is a prominent absorption on the blue side of the H $\alpha$ . We interpret it as due to Si II, since there is no evidence of high velocity hydrogen features in proximity other Balmer or Paschen lines. This absorption dip is not particularly strong in other *slow rising* type II SNe, although it was detected in SN 2009bw. Inserra et al. (2012) proposed it to be an evidence that SN 2009bw was interacting with the H-rich CSM already at early phases. However, for the reasons mentioned above, we do not find an unequivocal evidence of interaction in SN 2013ej - at least not before 30 days after explosion. Nonetheless, we can not rule out that signatures of interaction between SN ejecta and CSM may appear at later stages, since this was observed in a number of type II SNe (Chugai, Chevalier & Utrobin 2007). SN 2013ej shows an unusually slow rise to the light curve plateau. This property was observed only in the type IIP SN 2006bp and SN 2009bw. All of them are more luminous than normal SNe II (Pataf et al. 1994), but the statistics accumulated so far are poor. Through modeling (Zampieri et al. 2003; Pumo & Zampieri 2011), Inserra et al. (2012) estimated a progenitor mass of  $11\text{-}15 M_\odot$  for SN 2009bw. If the early spectroscopic and photometric similarities of SN 2013ej with SN 2009bw, are confirmed at late phases, this mass range should also be considered plausible in the case of SN 2013ej, and consistent with the progenitor mass inferred from the analysis of Fraser et al. (2013) ( $8\text{-}15.5 M_\odot$ ).

## ACKNOWLEDGMENTS

A.P., L.T. and S.B. are partially supported by the PRIN-INAF 2011 with the project "Transient Universe: from ESO Large to PESSTO". A.G. acknowledges support by the EU/FP7 via ERC grant n 307260, a GIF grant, and the Kimmel award. The research of JRM is funded through a Royal Society University Research Fellowship. Visiting Astronomer at the Infrared Telescope Facility, which is operated by the University of Hawaii under Cooperative Agreement no. NNX-08AE38A with the National Aeronautics and Space Administration, Science Mission Directorate, Planetary Astronomy Program. This paper is based on observations made with the following facilities: ESO NTT Telescope (program ID 188.D-3003), LCOGT 1m

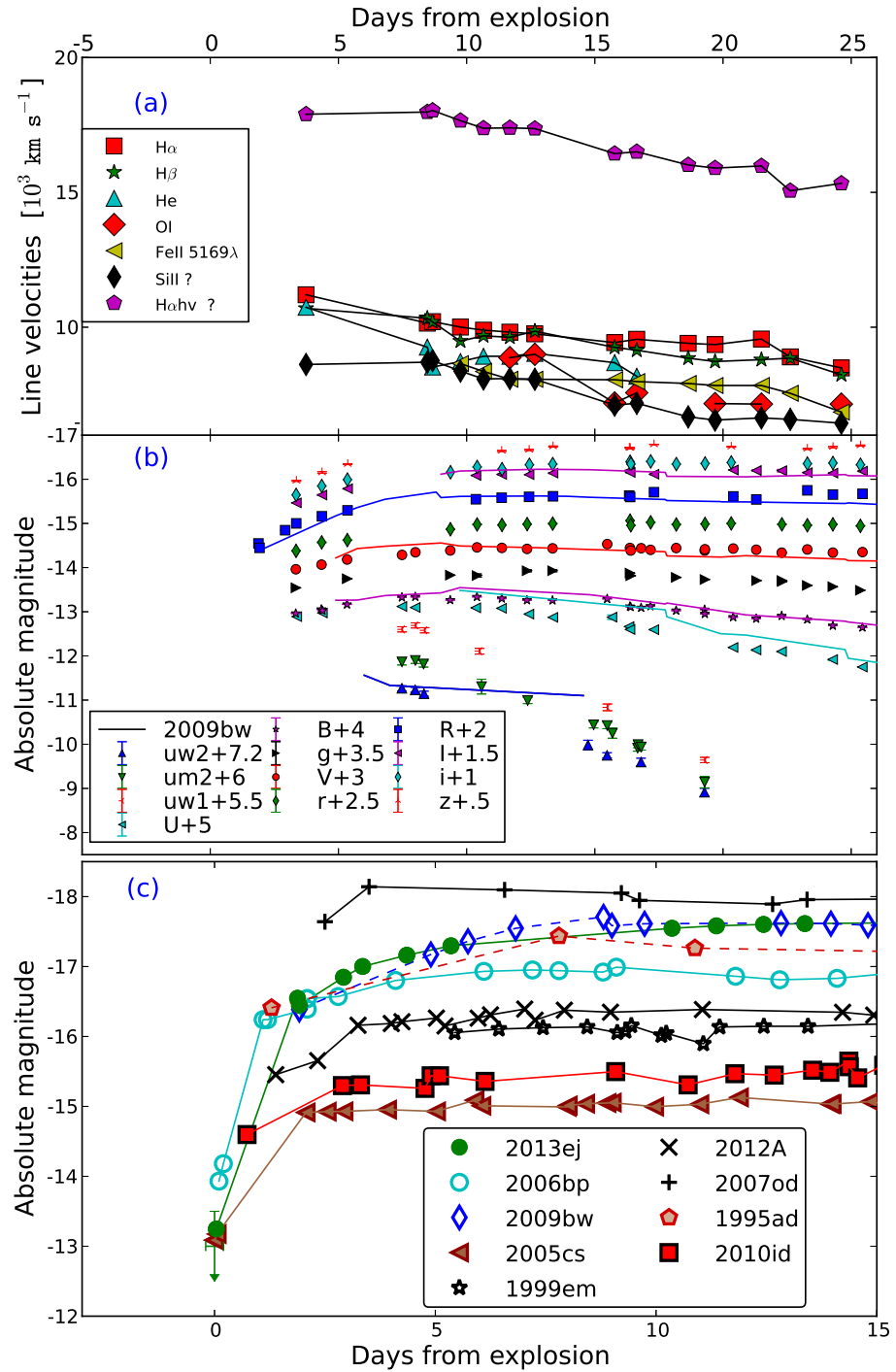


**Figure 2.** (a): Light curves of SN 2013ej in different bands (symbols), and comparison with the light curves of the twin SN 2009bw (solid lines). (b): Absolute R-band light curve of SN 2013ej compared with those of other type IIP SNe, including SN 2006bp, Quimby et al. 2007; SN 2009bw, Inserra et al. 2012; SN 2005cs Pastorello et al. 2006; SN 2007od, Inserra et al. 2011; SN 2012A, Tomasella et al. 2013, SN 1995ad, Inserra et al. 2013.

network of Telescopes (Haleakala, Siding Spring, Cerro Tololo, Mc Donald Observatory), NASA Infrared Telescope Facility (IRTF), 1.8m and 1.2m Telescopes (Asiago)

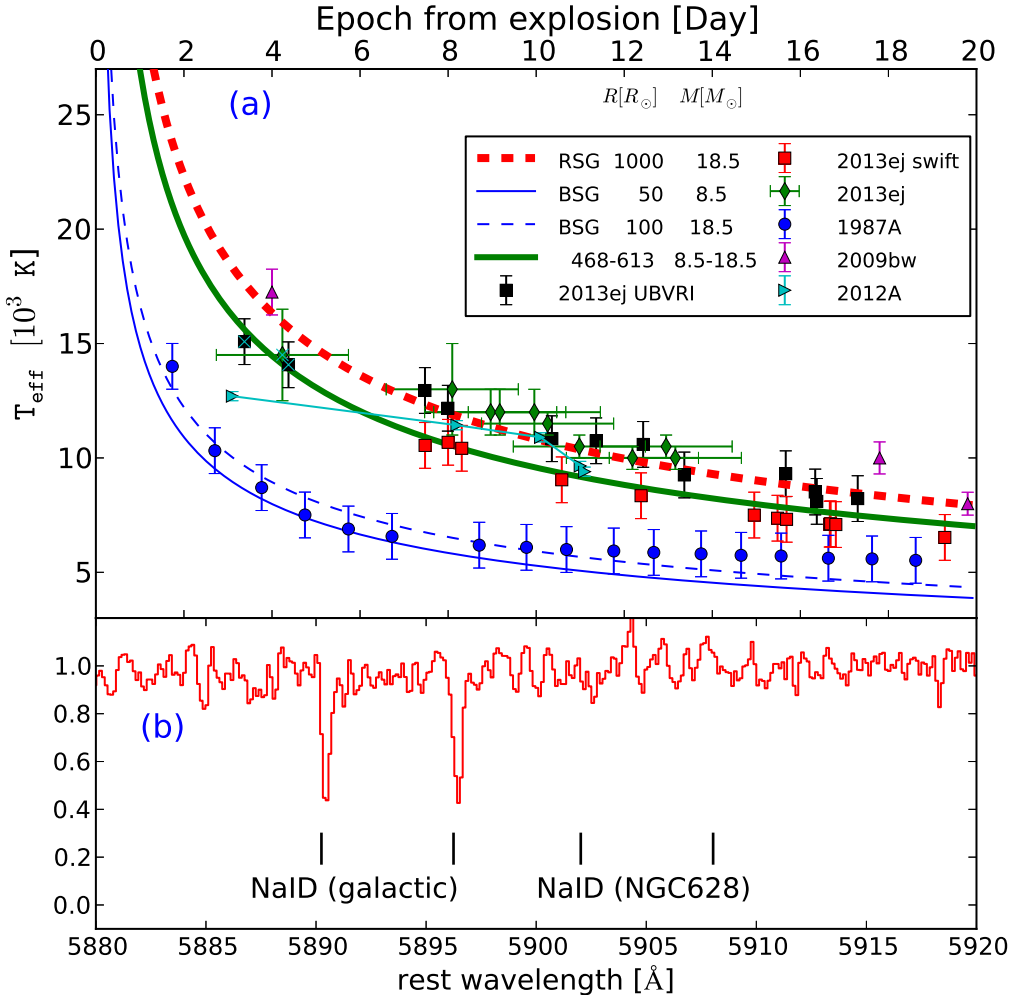


**Figure 3.** (a): Progenitor radius constraints using Rabinak & Waxman (2011) for RSG (red line), BSG (blue line) and 2013ej best fit (green line). Comparison objects: SN 1987A (Menzies et al. 1987), SN 2012A (Tomasella et al. 2013), SN 2009bw (Inserra et al. 2012); (b): Echelle spectrum of SN 2013ej obtained at the 1.8m asiago telescope on 24th August 2013. The Galactic NaID is clearly visible, while no NaID is detected at the redshift of M74. The x-axis is in the observed frame. (c): Photospheric velocity evolution for different elements in the ejecta of SN 2013ej.

## REFERENCES

- Baron E. et al., 2000, *The Astrophysical Journal*, 545, 444
- Brown P. J. et al., 2009, *The Astronomical Journal*, 137, 4517
- Brown . et al., 2013, eprint arXiv:1305.2437
- Chevalier R. A., Irwin C. M., 2011, *The Astrophysical Journal*, 729, L6
- Chugai N. N., Chevalier R. A., Utrobin V. P., 2007, *The Astrophysical Journal*, 662, 1136
- Cushing M., Vacca W., Rayner J., 2004, *Publications of the Astronomical Society of the Pacific*, 116, 362
- Dessart L., Hillier D. J., 2006, *Astronomy and Astrophysics*, 447, 691
- Fisher A. K., 2000, PhD thesis, THE UNIVERSITY OF OKLAHOMA
- Gal-Yam A. et al., 2011, *The Astrophysical Journal*, 736, 159
- Hamuy ., 2001, *ProQuest Dissertations And Theses: Thesis (Ph.D.)–The University of Arizona*
- Inserra C. et al., 2013, *Astronomy & Astrophysics*, 555
- Inserra C. et al., 2011, *Monthly Notices of the Royal Astronomical Society*, 417, 261
- Inserra C. et al., 2012, *Monthly Notices of the Royal Astronomical Society*, 422, 1122
- Kim . et al., 2013, *Central Bureau Electronic Telegrams*
- Landolt A. U., 1992, *The Astronomical Journal*, 104, 340
- Leonard D. C. et al., 2002, *Publications of the Astronomical Society of the Pacific*, 114, 35
- Menzies J. W. et al., 1987, *Monthly Notices of the Royal Astronomical Society*, 227, 39P

**Table 1.** Journal of spectroscopic observations.

Date	Telescope	JD −2,400,000 (days)	Phase <sup>a</sup> (days)	Instrument	Range (Å)	Resolution FWHM <sup>b</sup> (Å)
2013 Jul 27	IRTF	56501.1	4.1	SpeX	9000-25000	16/22/29
2013 Jul 27	FTS	56501.2	4.2	FLOYDS	3200-10000	5/12
2013 Jul 31	1.22m	56504.6	7.6	B&C	3400-8000	6.5
2013 Aug 01	FTN	56506	9.0	FLOYDS	3200-10000	6/13
2013 Aug 01	FTS	56506.2	9.2	FLOYDS	3200-10000	9/16
2013 Aug 02	FTN	56507	10	FLOYDS	3200-10000	6/13
2013 Aug 02	FTS	56507.3	10.3	FLOYDS	3200-10000	10/16
2013 Aug 03	FTN	56508	11	FLOYDS	3200-10000	6/13
2013 Aug 03	FTS	56508.2	11.2	FLOYDS	3200-10000	10/16
2013 Aug 04	FTS	56509.2	12.2	FLOYDS	3200-10000	9/15
2013 Aug 05	FTN	56510	12.9	FLOYDS	3200-10000	6/13
2013 Aug 05	FTS	56510.2	13.2	FLOYDS	3200-10000	10/17
2013 Aug 07	1.22m	56511.6	14.6	B&C	3400-8000	6.5
2013 Aug 08	1.22m	56512.5	15.5	B&C	3400-8000	6.5
2013 Aug 08	FTS	56513.3	16.3	FLOYDS	3200-10000	10/16
2013 Aug 09	FTS	56514.1	17.1	FLOYDS	3200-10000	9/14
2013 Aug 10	FTS	56514.1	17.1	FLOYDS	3200-10000	9/14
2013 Aug 11	FTS	56516.2	19.2	FLOYDS	3200-10000	10/17
2013 Aug 12	FTS	56517.2	20.2	FLOYDS	3200-10000	11/16
2013 Aug 13	FTS	56518.1	21.1	FLOYDS	3200-10000	11/17
2013 Aug 15	FTS	56520.1	23.1	FLOYDS	3200-10000	10/16
2013 Aug 17	NTT	56521.7	24.7	SOFI	9000-25000	20/40
2013 Aug 17	FTS	56522.1	25.1	FLOYDS	3200-10000	10/16
2013 Aug 21	1.8m	56526.42	29.4	Echelle	5800-6000	0.4

<sup>a</sup> Relative to the date of the estimate shock breakout (JD = 2456497.0).

<sup>b</sup> FWHM of night-sky emission lines.

- Pastorello A. et al., 2006, Monthly Notices of the Royal Astronomical Society, 370, 1752  
 Patat ., Barbon ., Cappellaro ., Turatto ., 1994, Astronomy and Astrophysics (ISSN 0004-6361), 282, 731  
 Pumo M. L., Zampieri L., 2011, The Astrophysical Journal, 741, 41  
 Quimby R. M., Wheeler J. C., Hoflich P., Akerlof C. W., Brown P. J., Rykoff E. S., 2007, The Astrophysical Journal, 666, 1093  
 Rabinak I., Waxman E., 2011, The Astrophysical Journal, 728, 63  
 Rayner J., Toomey D., Onaka P., Denault A., Stahlberger W., Vacca W., Cushing M., Wang S., 2003, Publications of the Astronomical Society of the Pacific, 115, 362  
 Roming P. W. A. et al., 2005, Space Science Reviews, 120, 95  
 Shappee B. J. et al., 2013, The Astronomer's Telegram  
 Smartt S. J., 2009, Annual Review of Astronomy & Astrophysics, 47, 63  
 Tomasella L. et al., 2013, Monthly Notices of the Royal Astronomical Society, -1, 1813  
 Vacca W., Cushing M., Rayner J., 2003, Publications of the Astronomical Society of the Pacific, 115, 389  
 Valenti . et al., 2013, Central Bureau Electronic Telegrams  
 Waxman E., Meszaros P., Campana S., 2007, The Astrophysical Journal, 667, 351  
 Zampieri L., Pastorello A., Turatto M., Cappellaro E., Benetti S., Altavilla G., Mazzali P., Hamuy M., 2003, Monthly Notices of the Royal Astronomical Society, 338, 711

**Table 2.** Photometric Data

Date	JD	mag	Filter	telescope <sup>a</sup>	Date	JD	mag	Filter	telescope <sup>a</sup>
2013-07-27	56500.333	13.077 0.014	B	1m0-04	2013-08-13	56517.391	12.896 0.018	U	1m0-04
2013-07-27	56500.338	13.019 0.015	V	1m0-04	2013-08-13	56517.396	13.160 0.015	B	1m0-04
2013-07-27	56500.354	12.946 0.018	R	1m0-04	2013-08-13	56517.398	12.550 0.015	V	1m0-04
2013-07-27	56500.357	12.941 0.021	I	1m0-04	2013-08-13	56517.400	12.335 0.019	R	1m0-04
2013-07-27	56500.374	12.198 0.016	U	1m0-04	2013-08-13	56517.402	12.197 0.023	I	1m0-04
2013-07-28	56501.333	12.986 0.017	B	1m0-04	2013-08-14	56518.290	12.953 0.018	U	1m0-04
2013-07-28	56501.338	12.914 0.019	V	1m0-04	2013-08-14	56518.295	13.196 0.015	B	1m0-04
2013-07-28	56501.354	12.784 0.023	R	1m0-04	2013-08-14	56518.297	12.577 0.021	V	1m0-04
2013-07-28	56501.357	12.764 0.026	I	1m0-04	2013-08-14	56518.299	12.404 0.027	R	1m0-04
2013-07-28	56501.374	12.114 0.017	U	1m0-04	2013-08-14	56518.301	12.209 0.027	I	1m0-04
2013-07-28	56501.375	13.015 0.017	B	1m0-08	2013-08-15	56519.283	12.989 0.022	U	1m0-09
2013-07-29	56502.333	12.874 0.014	B	1m0-04	2013-08-15	56519.288	13.133 0.024	B	1m0-09
2013-07-29	56502.338	12.798 0.016	V	1m0-09	2013-08-15	56519.290	12.643 0.032	V	1m0-09
2013-07-29	56502.354	12.650 0.016	R	1m0-09	2013-08-15	56519.293	12.212 0.046	I	1m0-09
2013-07-29	56502.357	12.621 0.019	I	1m0-09	2013-08-16	56520.286	13.214 0.016	B	1m0-09
2013-08-02	56506.358	12.775 0.013	B	1m0-04	2013-08-16	56520.288	12.570 0.021	V	1m0-09
2013-08-02	56506.362	12.593 0.014	V	1m0-04	2013-08-16	56520.290	12.198 0.037	R	1m0-09
2013-08-03	56507.356	11.999 0.017	U	1m0-08	2013-08-16	56520.292	12.257 0.023	I	1m0-09
2013-08-03	56507.361	12.399 0.022	R	1m0-08	2013-08-17	56521.278	13.169 0.020	U	1m0-05
2013-08-03	56507.363	12.320 0.020	I	1m0-08	2013-08-17	56521.282	13.355 0.018	B	1m0-05
2013-08-03	56507.401	12.703 0.021	B	1m0-08	2013-08-17	56521.285	12.642 0.017	V	1m0-05
2013-08-03	56507.404	12.523 0.022	V	1m0-08	2013-08-17	56521.287	12.293 0.022	R	1m0-05
2013-08-04	56508.361	12.009 0.017	U	1m0-08	2013-08-17	56521.288	12.268 0.026	I	1m0-05
2013-08-04	56508.366	12.365 0.019	R	1m0-08	2013-08-18	56522.433	13.340 0.025	U	1m0-08
2013-08-04	56508.367	12.298 0.020	I	1m0-08	2013-08-18	56522.438	13.395 0.020	B	1m0-08
2013-08-04	56508.371	12.739 0.014	B	1m0-08	2013-08-18	56522.441	12.630 0.023	V	1m0-08
2013-08-04	56508.374	12.535 0.018	V	1m0-08	2013-08-18	56522.442	12.276 0.026	R	1m0-08
2013-08-05	56509.353	12.779 0.014	B	1m0-08	2013-08-18	56522.444	12.222 0.026	I	1m0-08
2013-08-05	56509.356	12.558 0.018	V	1m0-08	2013-08-20	56524.340	13.538 0.023	U	1m0-05
2013-08-05	56509.429	12.141 0.017	U	1m0-08	2013-08-20	56524.344	13.555 0.018	B	1m0-05
2013-08-05	56509.434	12.344 0.023	R	1m0-08	2013-08-20	56524.347	12.745 0.022	V	1m0-05
2013-08-05	56509.436	12.303 0.020	I	1m0-08	2013-08-20	56524.349	12.512 0.020	R	1m0-05
2013-08-06	56510.349	12.782 0.020	B	1m0-08	2013-08-20	56524.351	12.344 0.020	I	1m0-05
2013-08-06	56510.352	12.545 0.023	V	1m0-08	2013-08-21	56525.300	13.667 0.034	U	1m0-08
2013-08-06	56510.364	12.215 0.022	U	1m0-08	2013-08-21	56525.305	13.590 0.022	B	1m0-08
2013-08-06	56510.369	12.333 0.027	R	1m0-08	2013-08-21	56525.308	12.748 0.023	V	1m0-08
2013-08-06	56510.370	12.268 0.025	I	1m0-08	2013-08-21	56525.309	12.534 0.028	R	1m0-08
2013-08-09	56513.337	12.424 0.020	U	1m0-08	2013-08-21	56525.311	12.223 0.032	I	1m0-08
2013-08-09	56513.341	12.316 0.023	R	1m0-08	2013-08-21	56525.314	13.658 0.021	U	1m0-09
2013-08-09	56513.343	12.214 0.027	I	1m0-08	2013-08-21	56525.319	13.580 0.015	B	1m0-09
2013-08-09	56513.367	12.920 0.015	B	1m0-08	2013-08-21	56525.321	12.739 0.017	V	1m0-09
2013-08-09	56513.370	12.537 0.021	V	1m0-08	2013-08-21	56525.323	12.453 0.023	R	1m0-09
2013-08-09	56513.373	12.489 0.016	U	1m0-04	2013-08-21	56525.324	12.231 0.018	I	1m0-09
2013-08-09	56513.378	12.347 0.018	R	1m0-04	2013-08-22	56526.318	13.812 0.023	U	1m0-04
2013-08-09	56513.380	12.252 0.023	I	1m0-04	2013-08-22	56526.321	13.666 0.015	B	1m0-04
2013-08-09	56513.397	12.932 0.015	B	1m0-04	2013-08-22	56526.324	12.788 0.020	V	1m0-04
2013-08-09	56513.400	12.594 0.018	V	1m0-04	2013-08-22	56526.326	12.516 0.023	R	1m0-04
2013-08-10	56514.171	12.914 0.016	B	1m0-10	2013-08-22	56526.327	12.238 0.021	I	1m0-04
2013-08-10	56514.173	12.579 0.015	V	1m0-10	2013-08-25	56529.295	14.087 0.027	U	1m0-04
2013-08-10	56514.303	12.493 0.072	U	1m0-09	2013-08-25	56529.300	13.829 0.016	B	1m0-04
2013-08-10	56514.307	12.240 0.020	R	1m0-09	2013-08-25	56529.303	12.920 0.016	V	1m0-04
2013-08-10	56514.309	12.293 0.023	I	1m0-09	2013-08-25	56529.305	12.579 0.019	R	1m0-04
2013-08-11	56515.171	13.011 0.015	B	1m0-13	2013-08-25	56529.306	12.465 0.026	I	1m0-04
2013-08-11	56515.174	12.538 0.016	V	1m0-13	2013-08-29	56533.428	14.389 0.029	U	1m0-08
2013-08-12	56516.291	13.089 0.014	B	1m0-04	2013-08-29	56533.433	14.005 0.022	B	1m0-08
2013-08-12	56516.294	12.566 0.014	V	1m0-04	2013-08-29	56533.435	12.927 0.020	V	1m0-08

<sup>a</sup> 1m0-08 (McDonald observatory, USA); 1m0-10, 1m0-12, 1m0-13 (Sutherland, South Africa), 1m0-04, 1m0-05, 1m0-09 (Cerro Tololo, Chile); 1m0-03, 1m0-11 (Siding Spring, Australia)

**Table 3.** ...continued

Date	JD	mag	Filter	telescope <sup>a</sup>	Date	JD	mag	Filter	telescope <sup>a</sup>		
2013-08-29	56533.437	12.608	0.028	R	1m0-08	2013-08-17	56521.288	12.652	0.031	zs	1m0-04
2013-08-29	56533.439	12.416	0.031	I	1m0-08	2013-08-18	56522.357	13.035	0.020	gp	1m0-08
2013-08-30	56534.323	14.428	0.027	U	1m0-08	2013-08-18	56522.359	12.513	0.019	rp	1m0-08
2013-08-30	56534.328	14.028	0.019	B	1m0-08	2013-08-18	56522.361	12.590	0.020	ip	1m0-08
2013-08-30	56534.331	12.957	0.022	V	1m0-08	2013-08-18	56522.362	12.617	0.024	zs	1m0-08
2013-07-27	56500.341	12.980	0.015	gp	1m0-04	2013-08-20	56524.327	14.841	0.035	up	1m0-05
2013-07-27	56500.346	13.079	0.019	rp	1m0-04	2013-08-20	56524.331	13.175	0.017	gp	1m0-05
2013-07-27	56500.349	13.272	0.019	ip	1m0-04	2013-08-20	56524.334	12.615	0.018	rp	1m0-05
2013-07-27	56500.360	13.418	0.024	zs	1m0-04	2013-08-20	56524.336	12.631	0.022	ip	1m0-05
2013-07-28	56501.346	12.886	0.022	rp	1m0-04	2013-08-21	56525.307	14.782	0.046	up	1m0-04
2013-07-28	56501.349	13.071	0.022	ip	1m0-04	2013-08-21	56525.311	13.191	0.017	gp	1m0-04
2013-07-28	56501.360	13.228	0.033	zs	1m0-04	2013-08-21	56525.314	12.568	0.019	rp	1m0-04
2013-07-29	56502.341	12.774	0.014	gp	1m0-09	2013-08-21	56525.316	12.613	0.020	ip	1m0-04
2013-07-29	56502.346	12.835	0.017	rp	1m0-09	2013-08-21	56525.317	12.636	0.024	zs	1m0-04
2013-07-29	56502.349	12.927	0.021	ip	1m0-09	2013-08-22	56526.304	15.066	0.072	up	1m0-09
2013-07-29	56502.360	13.038	0.023	zs	1m0-09	2013-08-22	56526.311	12.594	0.027	rp	1m0-09
2013-08-02	56506.363	12.693	0.013	gp	1m0-04	2013-08-22	56526.313	12.618	0.023	ip	1m0-09
2013-08-02	56506.366	12.590	0.014	rp	1m0-04	2013-08-22	56526.314	12.635	0.033	zs	1m0-09
2013-08-02	56506.369	12.760	0.015	ip	1m0-04	2013-08-25	56529.296	15.080	0.030	up	1m0-09
2013-08-03	56507.405	12.702	0.057	gp	1m0-08	2013-08-25	56529.300	13.377	0.020	gp	1m0-09
2013-08-03	56507.408	12.481	0.020	rp	1m0-08	2013-08-25	56529.303	12.646	0.023	rp	1m0-09
2013-08-03	56507.410	12.640	0.019	ip	1m0-08	2013-08-25	56529.304	12.679	0.026	ip	1m0-09
2013-08-04	56508.369	12.741	0.024	zs	1m0-08	2013-08-25	56529.306	12.666	0.027	zs	1m0-09
2013-08-04	56508.378	12.492	0.018	rp	1m0-08	2013-08-29	56533.459	13.494	0.024	gp	1m0-08
2013-08-04	56508.380	12.690	0.022	ip	1m0-08	2013-08-29	56533.461	12.750	0.024	rp	1m0-08
2013-08-05	56509.357	12.593	0.041	gp	1m0-08	2013-08-29	56533.463	12.753	0.022	ip	1m0-08
2013-08-05	56509.360	12.473	0.022	rp	1m0-08	2013-08-29	56533.465	12.759	0.032	zs	1m0-08
2013-08-05	56509.437	12.717	0.027	zs	1m0-08	2013-07-31	56504.481	12.238	0.059	uvw2	swift
2013-08-05	56509.448	12.591	0.021	ip	1m0-08	2013-07-31	56504.473	11.717	0.057	uvw1	swift
2013-08-06	56510.353	12.592	0.041	gp	1m0-08	2013-07-31	56504.476	12.538	0.070	uvw2	swift
2013-08-06	56510.356	12.463	0.023	rp	1m0-08	2013-08-01	56505.006	12.149	0.058	uvw2	swift
2013-08-06	56510.358	12.575	0.023	ip	1m0-08	2013-08-01	56504.993	11.752	0.056	uvw1	swift
2013-08-06	56510.372	12.640	0.026	zs	1m0-08	2013-08-01	56504.999	12.505	0.069	uvw2	swift
2013-08-09	56513.345	12.667	0.026	zs	1m0-08	2013-08-01	56505.362	12.259	0.058	uvw2	swift
2013-08-09	56513.371	12.647	0.024	gp	1m0-08	2013-08-01	56505.335	11.839	0.057	uvw1	swift
2013-08-09	56513.374	12.395	0.022	rp	1m0-08	2013-08-01	56505.319	12.585	0.071	uvw2	swift
2013-08-09	56513.376	12.522	0.021	ip	1m0-08	2013-08-03	56507.499	12.734	0.075	uvw2	swift
2013-08-09	56513.381	12.676	0.027	zs	1m0-04	2013-08-03	56507.582	13.098	0.070	uvw2	swift
2013-08-09	56513.401	12.706	0.019	gp	1m0-04	2013-08-05	56509.381	13.413	0.070	uvw2	swift
2013-08-09	56513.404	12.500	0.018	rp	1m0-04	2013-08-07	56511.734	13.000	0.059	uvw1	swift
2013-08-09	56513.406	12.572	0.027	ip	1m0-04	2013-08-07	56511.953	13.962	0.072	uvw2	swift
2013-08-10	56514.178	12.433	0.019	rp	1m0-10	2013-08-08	56512.477	13.235	0.087	uvw1	swift
2013-08-10	56514.179	12.514	0.022	ip	1m0-10	2013-08-08	56512.490	14.005	0.060	uvw2	swift
2013-08-10	56514.310	12.594	0.024	zs	1m0-09	2013-08-08	56512.482	13.979	0.113	uvw2	swift
2013-08-11	56515.175	12.743	0.015	gp	1m0-13	2013-08-08	56512.687	14.154	0.070	uvw2	swift
2013-08-11	56515.178	12.482	0.016	rp	1m0-13	2013-08-09	56513.669	14.490	0.071	uvw2	swift
2013-08-11	56515.179	12.575	0.018	ip	1m0-13	2013-08-09	56513.688	14.411	0.071	uvw2	swift
2013-08-12	56516.296	12.791	0.014	gp	1m0-04	2013-08-09	56513.801	13.387	0.089	uvw1	swift
2013-08-12	56516.298	12.470	0.014	rp	1m0-04	2013-08-09	56513.806	14.464	0.129	uvw2	swift
2013-08-12	56516.300	12.562	0.018	ip	1m0-04	2013-08-12	56516.277	14.070	0.107	uvw1	swift
2013-08-13	56517.312	13.820	0.049	up	1m0-04	2013-08-12	56516.282	15.261	0.168	uvw2	swift
2013-08-13	56517.320	12.458	0.014	rp	1m0-04	2013-08-12	56516.290	15.197	0.065	uvw2	swift
2013-08-13	56517.322	12.539	0.015	ip	1m0-04	2013-07-31	56504.474	11.968	0.241	U	swift
2013-08-13	56517.323	12.645	0.019	zs	1m0-04	2013-07-31	56504.475	12.714	0.062	B	swift
2013-08-14	56518.307	12.815	0.021	gp	1m0-04	2013-07-31	56504.478	12.694	0.043	V	swift
2013-08-15	56519.294	12.814	0.023	gp	1m0-04	2013-08-01	56504.995	11.991	0.282	U	swift
2013-08-15	56519.297	12.478	0.023	rp	1m0-04	2013-08-01	56504.996	12.700	0.045	B	swift
2013-08-15	56519.308	12.836	0.018	gp	1m0-08	2013-08-02	56505.002	12.634	0.037	V	swift
2013-08-16	56520.287	12.926	0.014	gp	1m0-05	2013-08-08	56512.481	12.747	0.096	B	swift
2013-08-16	56520.289	12.499	0.018	rp	1m0-05	2013-08-08	56512.484	12.449	0.065	V	swift
2013-08-16	56520.291	12.565	0.021	ip	1m0-05	2013-08-08	56512.668	12.210	0.049	U	swift
2013-08-16	56520.292	12.693	0.024	zs	1m0-05	2013-08-09	56513.805	12.948	0.090	B	swift
2013-08-17	56521.282	12.954	0.021	gp	1m0-04	2013-08-09	56513.808	12.542	0.067	V	swift
2013-08-17	56521.285	12.479	0.024	rp	1m0-04	2013-08-12	56516.281	12.991	0.083	B	swift
2013-08-17	56521.287	12.550	0.026	ip	1m0-04	2013-08-12	56516.284	12.596	0.066	V	swift